

Aspect of Floquet physics in closed quantum systems

K. Sengupta

IACS, Kolkata

Collaborators

Tista Banerjee, IACS, Kolkata

PRL 130, 120401 (2024)

Sayan Choudhury, HRI Allahabad

PRB 109 214304 (2024)

Indrani Paul, LMPQ, Paris

arXiv:2404.06536

Somsubhra Ghosh, IACS, Kolkata

arXiv:2407.20764

Outline

Driven systems: Thermalization

Prethermal Physics: emergent symmetry

Prethermal Hilbert space fragmentation

Arresting heating: a brief introduction

Two-rate periodic protocol

Future directions.

Consider a generic state of quantum non-integrable many-body system



$$|\psi(t)\rangle = \sum_m C_m e^{-iE_m t} |m\rangle,$$

D'Alessio et. al
Adv. Phys. 65, 239 (2016)

The time evolution of a generic operator for this state is given by

$$\begin{aligned} O(t) &\equiv \langle \psi(t) | \hat{O} | \psi(t) \rangle = \sum_{m,n} C_m^* C_n e^{i(E_m - E_n)t} O_{mn} \\ &= \sum_m |C_m|^2 O_{mm} + \sum_{m,n \neq m} C_m^* C_n e^{i(E_m - E_n)t} O_{mn} \end{aligned}$$

$$O_{mn} = \langle m | \hat{O} | n \rangle.$$

Issues with long-time behavior:

- a) The steady state value of $O(t)$ depends on the overlap coefficients: no thermalization (in the sense that the value does not agree with standard ME prediction)**
- a) It takes an incredibly long time to reach the steady state (predicts a very large relaxation time).**

Invoking random matrix theory remedies these problems since within RMT $O_{mm} = O'$ and $O_{mn} = 0$. However it provides an energy independent answer which does not agree with standard numerical results.

Eigenstate Thermalization Hypothesis

Generalization of the RMT result for the matrix elements of a “typical” operator

$$O_{mn} = O(\bar{E})\delta_{mn} + e^{-S(\bar{E})/2} f_O(\bar{E}, \omega) R_{mn}, \quad \bar{E} \equiv (E_m + E_n)/2,$$

Both O and f_O are smooth functions of their arguments, S is the entropy, and R is a gaussian random number.

It states that for a large-enough system, the answer is nearly identical to that obtained using a microcanonical ensemble at the average energy.

$$\bar{O} \equiv \lim_{t_0 \rightarrow \infty} \frac{1}{t_0} \int_0^{t_0} dt O(t) = \sum_m |C_m|^2 O_{mm} = \text{Tr}[\hat{\rho}_{\text{DE}} \hat{O}], \quad O_{\text{ME}} = \text{Tr}[\hat{\rho}_{\text{ME}} \hat{O}]$$

$$\bar{O} \simeq O(\langle E \rangle) \simeq O_{\text{ME}}.$$

This relies on the fact that energy fluctuations in a many-body system are subextensive.

$$O_{mm} \approx O(\langle E \rangle) + (E_m - \langle E \rangle) \left. \frac{dO}{dE} \right|_{\langle E \rangle} + \frac{1}{2} (E_m - \langle E \rangle)^2 \left. \frac{d^2 O}{dE^2} \right|_{\langle E \rangle},$$

$$\bar{O} \approx O(\langle E \rangle) + \frac{1}{2} (\delta E)^2 O''(\langle E \rangle) \approx O_{\text{ME}} + \frac{1}{2} [(\delta E)^2 - (\delta E_{\text{ME}})^2] O''(\langle E \rangle),$$

Floquet version: ETH in a periodically driven system

Periodic drive: Stroboscopic dynamics is completely determined by the Floquet Hamiltonian: $U(nT,0) = \exp[-i H_F nT]$

For low or intermediate drive frequency, H_F can not be typically described by a short range Hamiltonian

The Floquet eigenvalues are uniformly distributed over the first Floquet Brillouin zone [Rigol et al, PRX (2014)]

At long times, the system heats up to infinite temperature: rapid growth of entanglement entropy to its maximum value.

However, at high drive frequencies the thermalization timescale are exponentially large [T. Mori et al, PRL 2016]

This makes prethermal regime experimentally relevant.

These regimes show several phenomena which do not have equilibrium analogue.

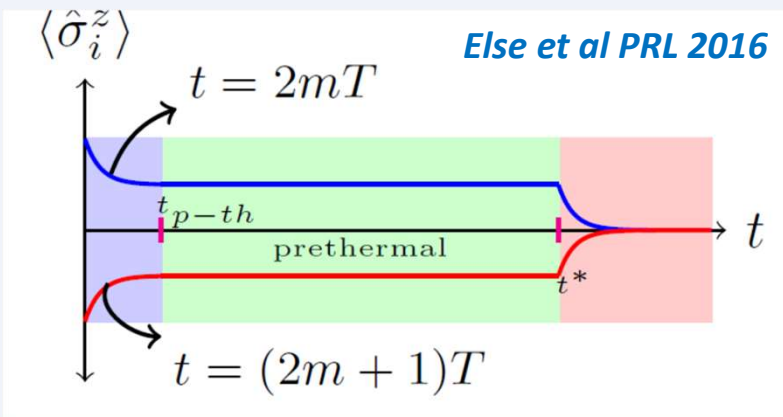
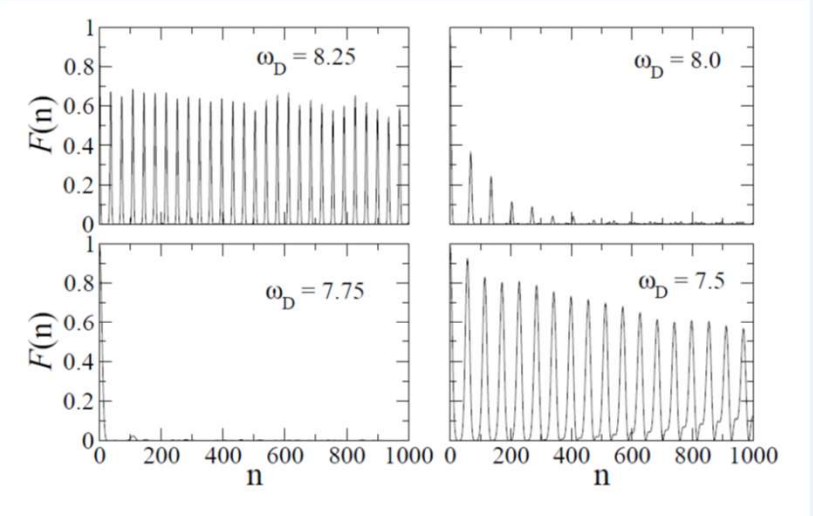
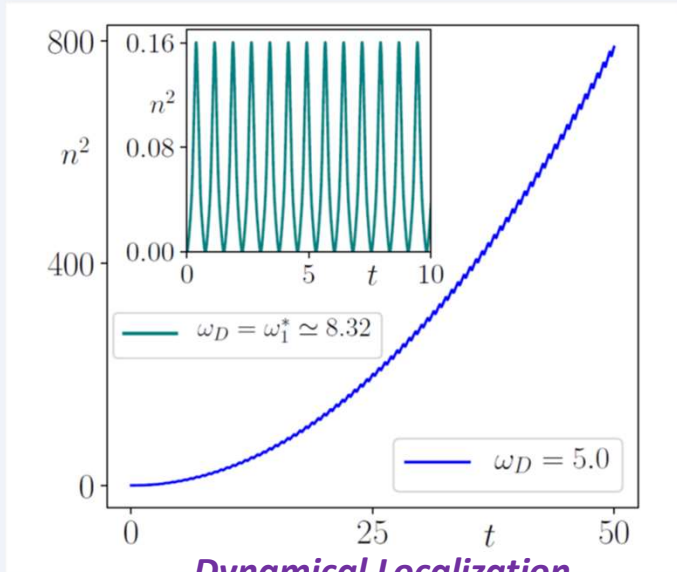
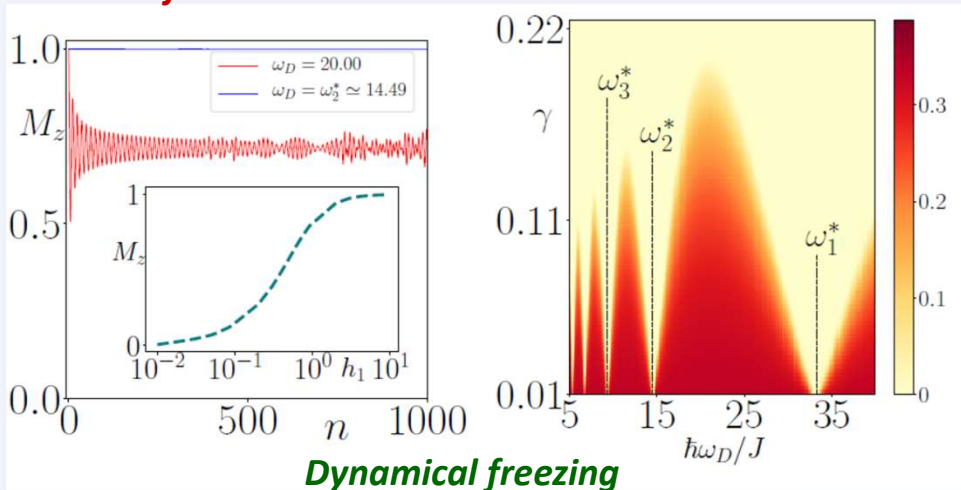
Many of these phenomena can be understood to be the result of approximate emergent symmetries of driven systems.

Prethermal physics and emergent symmetry

Banerjee et al arXiv 2024

Prethermal phenomena

Refael et al. Scipost Phys. 2018



Scar induced oscillations Mukherjee et al PRB 2020

Prethermal discrete time crystal

Emergent symmetry

Banerjee et al arXiv 2024

Most of these prethermal phenomenon can be understood as a consequence of an approximate emergent symmetry



The first order Floquet Hamiltonian, computed in some approximation scheme commutes with some operator O at special drive frequencies.



As long as the first order Floquet Hamiltonian controls the dynamics, $\langle O \rangle$ is approximately conserved at these frequencies. This happens till a prethermal timescale $\sim \exp[c \omega_d]$



For time crystals, the argument requires a slight modification.

Example of driven Ising model.

$$H_{\text{Ising}} = -J \sum_{\langle \ell j \rangle} \sigma_\ell^x \sigma_j^x - h_0 \sum_j \sigma_j^z$$

$$h_0(t) = h_s + h_1 \cos \omega_D t + i\gamma,$$



Jordan Wigner

$$H = 2 \sum_{k \in \text{BZ}/2} \psi_k^\dagger H_k \psi_k$$

$$H_k = \tau_z (h_0(t) - \cos ka + i\gamma) + \tau_x \sin ka$$

$$H_F^{(1)} = 2 \sum_{k \in \text{BZ}/2} \left[\tau_z (h_s - \cos ka + i\gamma) + \tau_x J_0(\mu) \sin ka \right]$$

$$H_F^{(2)} = \sum_k \left[-4\tau_z \sin^2 ka \sum_{n=0}^{\infty} \frac{J_0(\mu) J_{2n+1}(\mu)}{(2n+1)\hbar\omega_D} + \tau_x \sin ka (h_s - \cos ka + i\gamma) \sum_{n=0}^{\infty} \frac{4J_{2n+1}(\mu)}{(2n+1)\hbar\omega_D} \right]$$

At special frequencies $H_F^{(1)}$ commutes with the magnetization

$$M_z = \sum_j \sigma_j^z$$

Dynamical freezing of magnetization

A. Das, PRB 2010.

Strong Hilbert space fragmentation

Hilbert space fragmentation: Introduction

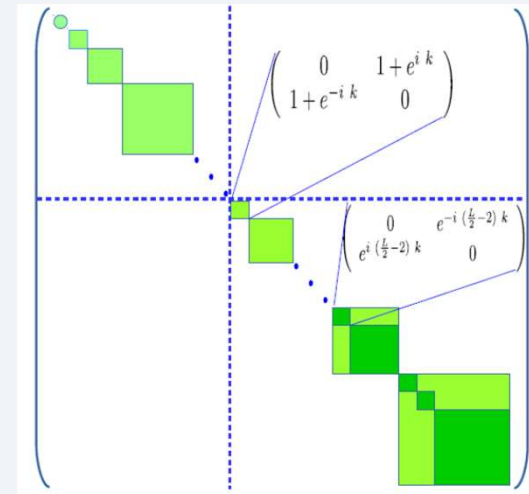
Breakdown of the Hilbert space into an exponentially large number of dynamically disconnected sectors.

The fragmentation is usually observed in the computational basis; classical Fock states such as number basis states $|n_1, n_2, \dots, n_j, \dots, n_L\rangle$

Such a separation of Hilbert space in dynamically disconnected sectors is different from those due to global symmetries; in the latter case number of sectors scale algebraically with L .

For strong Hilbert space fragmentation (HSF), with n being the largest fragment and N being the total Hilbert space dimensions, $n/N \sim e^{-L}$

Most of the model exhibiting strong HSF are 1D models; More recently a few higher dimensional models have been put forth (see for example, *Scipost Phys.* 14, 146 (2023)).



Signatures of strong HSF

1. Memory retainment leading to finite value of the autocorrelation function at long times
2. Deviation of the entanglement entropy from its symmetry resolved Page value.

A model of strong HSF

Tomasi et. al PRB 100, 214313 (2019)

Fermionic model with correlated hopping

$$\hat{H}_\infty = -t \sum_x \hat{P}_x (\hat{c}_{x+1}^\dagger \hat{c}_x + h.c.) \hat{P}_x$$

$$\hat{P}_x = 1 - (\hat{n}_{x+2} - \hat{n}_{x-1})^2, \quad \hat{P}_x^2 = \hat{P}_x,$$

Conservation: The conserved quantities are
 i) the fermionic charge N and
 ii) the number of bonds N_b with two occupied sites

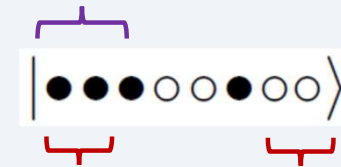


The largest symmetry sector corresponds to $N=L/2$ and $N_b=L/4$

The presence of these conserved quantities leads to exponentially many frozen states: $N_f \sim (1.62)^L / L^{1/2}$



Adjacent particle defects



Particle defect

Hole defect

There are (dynamical) states in this sector which has no overlap with a frozen states. Thus even within a symmetry sector, states are dynamically disconnected.



Number of particle and hole defects are separately conserved.
 The parity of the starting defect sites are conserved.

Counting of fragmentation

A: Number of states in the largest symmetry sector:

We need to fill L sites with $L/2$ particles and $L/4$ bonds

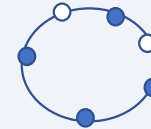
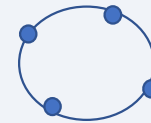
To do this first fill $L/2$ sites with particles keeping $L/2$ bonds

Next we insert $L/4$ empty sites so as to break $L/4$ of these $L/2$ bonds. This can be done in ${}^{L/2}C_{L/4}$ ways

Next, one needs to insert $L/4$ more empty sites without breaking any bonds. This can be done in ${}^{L/2-1}C_{L/4}$ ways.

Finally one gets a factor of 2 due to particle-hole inversion

Example for $L=8$



$$N_1 = 2 {}^{L/2-1}C_{L/4} {}^{L/2}C_{L/4} = ({}^{L/2}C_{L/4})^2 \sim 2^L/L$$

Dimension of the largest fragment

Start from an initial state for which $N_b = L/4$ such that there are $N_d = L/4$ particle and hole defects. This also leaves $P = L/4 - 1$ particle-hole pairs.

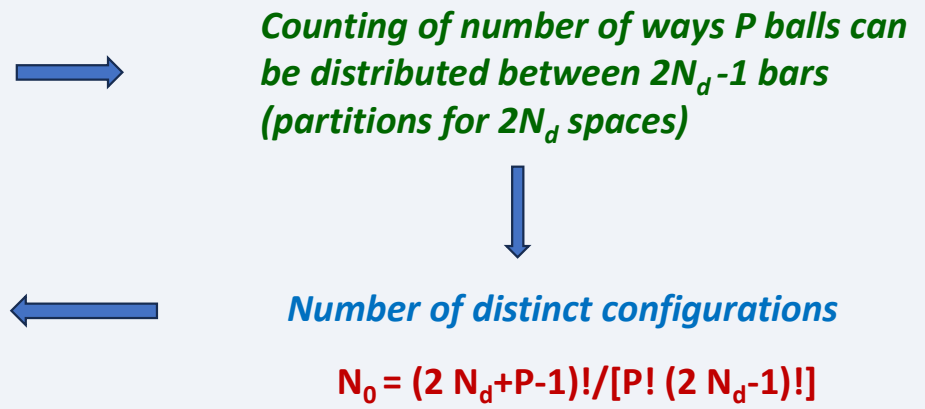
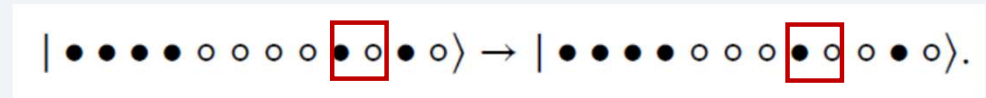
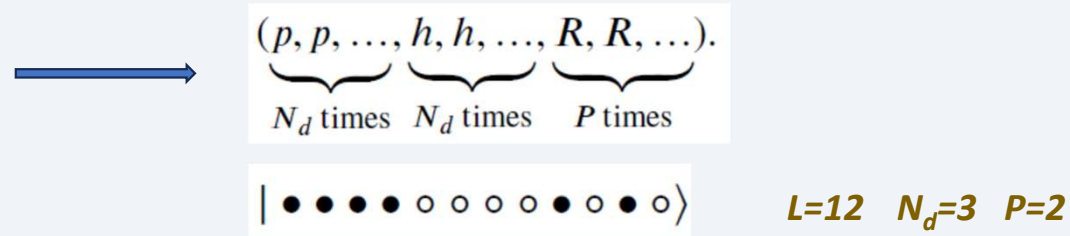
For half-filling one has $P = L/2 - (N_d + 1)$

Starting from this initial state the action of H leads to diffusion of particle from R to the sequence of hole defects. Such diffusion needs an accompanying hole motion and thus leads to pair movement.

The number of possible configurations obtained by action of H is the number of ways P pairs can be distributed among $2 N_d$ empty space between particle and hole defects.

Total number of such configurations is $N_t = L N_0 / 2$.

For large L and $L/4$ particle and hole defects, one has $N_t / N_1 \sim (0.8)^L$



Prethermal signature of strong fragmentation

Driving a spinless fermion chain: Numerics

We start from a fermion chain and drive the interaction term

For a square pulse protocol

$$[V(t) = -(+)V_1 \text{ for } t \leq (>)T/2]$$



The time evolution operator

$$U^s(T, 0) = e^{-iH_+T/2\hbar} e^{-iH_-T/2\hbar}$$



Can be expressed in terms of eigenvalues and eigenfunctions of H_+ and H_-

$$U^s(T, 0) = \sum_{m,n} c_{mn}^{+-} e^{-i(\epsilon_m^+ + \epsilon_n^-)T/2\hbar} |\xi_m^+\rangle \langle \xi_n^-| \quad c_{mn}^{+-} = \langle \xi_m^+ | \xi_n^- \rangle.$$

$$H_0(t) = V(t) \sum_{j=1..L} \hat{n}_j \hat{n}_{j+1}$$

$$H_1 = \sum_{j=1..L} -J(c_j^\dagger c_{j+1} + \text{H.c.}) + \hat{n}_j (V_0 \hat{n}_{j+1} + V_2 \hat{n}_{j+2})$$

For a continuous protocol

$$[V(t) = V_1 \cos \omega_D t]$$



The time evolution operator requires Suzuki-Trotter decomposition of U

$$U = \prod_j \exp[-i H_j \Delta t / \hbar] \quad \Delta t = T/N$$



U can be expressed in terms of eigenvalues and eigenfunctions of H_j

$$U^c(T, 0) = \prod_{j=1..N} \sum_n e^{-i\epsilon_n^j T/\hbar} |\xi_n^j\rangle \langle \xi_n^j|$$

This procedure allows one to numerically compute the exact Floquet Hamiltonian for the system

$$U = \exp[-iH_F T/\hbar]$$

Perturbative Analytics: Floquet perturbation theory

We consider a Hamiltonian $H(t) = H_0(t) + V(t)$ and construct the evolution operator U_0 corresponding to the largest term of the Hamiltonian $[H_0(t)]$

$$i\hbar \frac{\partial U_0(t, 0)}{\partial t} = H_0(t)U_0(t, 0).$$

Next, we construct states in the interaction picture and construct the corresponding Schrodinger equation

$$\psi^I(t) = U_0(0, t)\psi(t). \quad i\hbar \frac{\partial \psi^I}{\partial t} = V^I(t)\psi^I(t),$$

$$V^I(t) = U_0(0, t)VU_0(t, 0).$$

The evolution operator in the interaction picture reads

$$U^I(t, 0) = \mathcal{T}e^{-(i/\hbar) \int_0^t dt' V^I(t')}, \quad i\hbar \frac{\partial U^I(t, 0)}{\partial t} = V^I(t)U^I(t, 0).$$

U^I has the solution

$$U^I(t, 0) = I + \left(\frac{-i}{\hbar}\right) \int_0^t dt' V^I(t') \\ + \left(\frac{-i}{\hbar}\right)^2 \int_0^t dt_1 V^I(t_1) \int_0^{t_1} dt_2 V^I(t_2) + \dots$$

The perturbative evolution operator is given by $U(t, 0) = U_0(t, 0)U^I(t, 0).$

The method reduces to the usual rotating wave approximation when the drive term is the one with largest amplitude

Driven Fermi chain

Consider a chain of spinless fermions with nearest neighbor hopping and density-density interactions



$$H = -J \sum_j (c_j^\dagger c_{j+1} + \text{h.c.}) + V_1 \sum_j \hat{n}_j \hat{n}_{j+1} + V_2 \sum_j \hat{n}_j \hat{n}_{j+2}$$

We drive the chain by making $V_1 = V_1(t)$ a periodic function of time characterized by an amplitude V_1 and frequency $\omega_D = 2\pi/T$, Where T is the time period of the drive



$$V_1(t) = V_0 + V_1 \cos \omega_D t \quad \text{for cosine drive}$$

$$V_1(t) = V_0 + (-)^j V_1 \text{ for } t \in [jT/2, (j+1)T/2) \quad \text{for square pulse}$$

In the high drive amplitude regime, $V_1 \gg V_0, V_2, J$, one can obtain the Floquet Hamiltonian using FPT

$$H_F^{(1)} = \sum_{j=1..L} \hat{n}_j (V_0 \hat{n}_{j+1} + V_2 \hat{n}_{j+2}) - J \sum_{i=1..L} [(1 - \hat{A}_i^2) + f(\gamma_0) \hat{A}_i^2] c_i^\dagger c_{i+1} + \text{H.c.},$$

$$\hat{A}_j = (\hat{n}_{j+2} - \hat{n}_{j-1}), \quad \gamma_0 = V_1 T / (4\hbar)$$

$$f(\gamma_0) = J_0[2\gamma_0/\pi] \quad \text{Cosine protocol}$$

$$f(\gamma_0) = \gamma_0^{-1} \sin \gamma_0 \exp[i\gamma_0 A_j] \quad \text{Square Pulse protocol}$$

Realization of a Hamiltonian hosting HSF within first order Floquet at frequencies for which $f(T)=0$

$$\begin{aligned}\omega_m^* &= V_1/(\hbar\zeta_m) \quad \text{for cosine protocol} \\ &= V_1/(2\hbar m) \quad \text{for square-pulse protocol.}\end{aligned}$$



$$\begin{aligned}H_F^{(1)} &= \sum_{j=1..L} \hat{n}_j (V_0 \hat{n}_{j+1} + V_2 \hat{n}_{j+2}) \\ &\quad - J \sum_{j=1..L} [(1 - \hat{A}_j^2) \cdot c_j^\dagger c_{j+1} + \text{H.c.},\end{aligned}$$

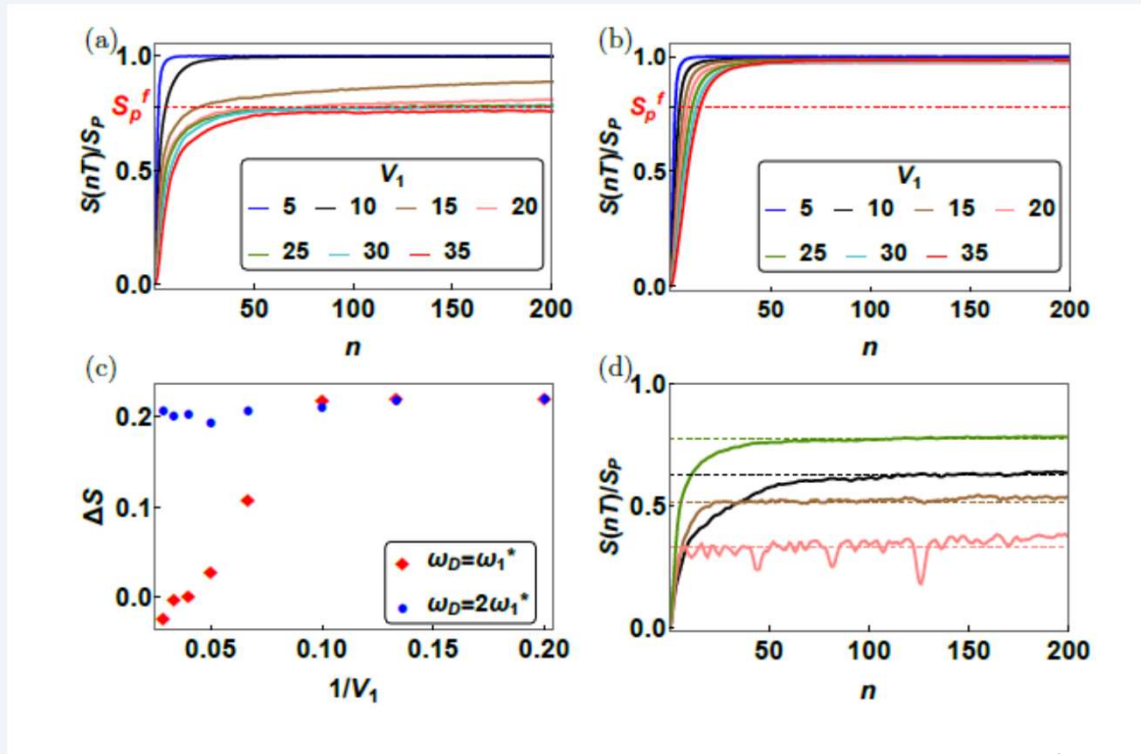
Higher order terms is expected to destroy the fragmentation.

However for large drive amplitudes such terms are small.

This leads to a large prethermal region where signatures of HSF can be seen.

The extent of the prethermal regime showing signatures of HSF can be controlled by tuning drive parameters

Entanglement entropy of the driven chain: Square-pulse protocol



$$S_p = \ln D_{\text{system}} - 1/2$$

$$S_p^f = \ln D_{\text{fragment}} - 1/2$$

(a bit more complicated for symmetry-resolved sectors)

Entanglement entropy saturates to the Page value of the sector (S_p^f) instead of that of the system (S_p) at special drive frequencies for an exponentially large prethermal timescale

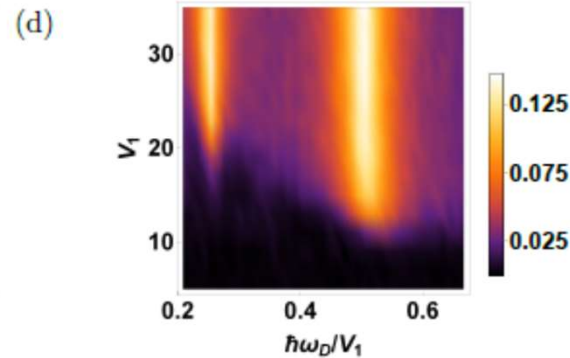
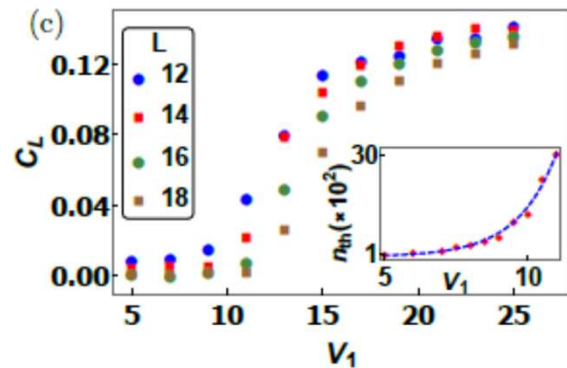
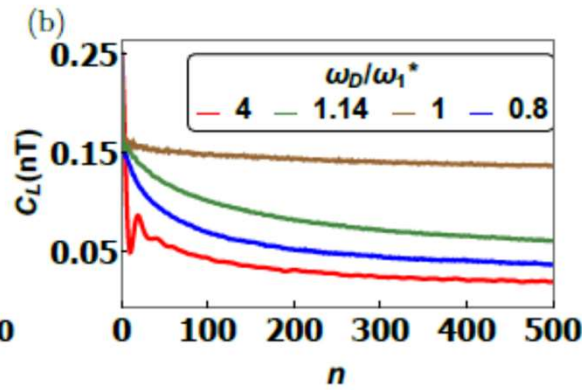
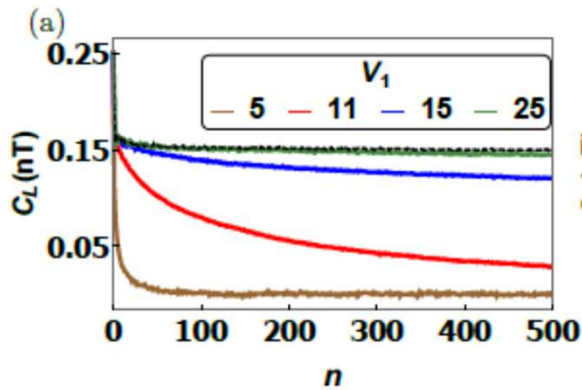
Entanglement entropy saturates to an Initial state dependent value.

Signature of prethermal HSF.

Fermion density-density autocorrelators: Square pulse protocol

$$C_L(nT) = \langle (n_{L/2}(nT) - 1/2) (n_{L/2}(0) - 1/2) \rangle$$

L=16



The system retains memory of the initial state for the large number of drive cycles

Thermalization time and hence the extent of the prethermal regime increases exponentially as a function of the drive amplitude showing stability of prethermal fragmentation.

Near the threshold value, the extent of the prethermal regime grows exponentially with drive amplitude

Dynamics of the frozen state: Continuous protocol

$$\chi_j(nT) = \langle \psi_f(nT) | \hat{n}_j \hat{n}_{j+2} | \psi_f(nT) \rangle$$

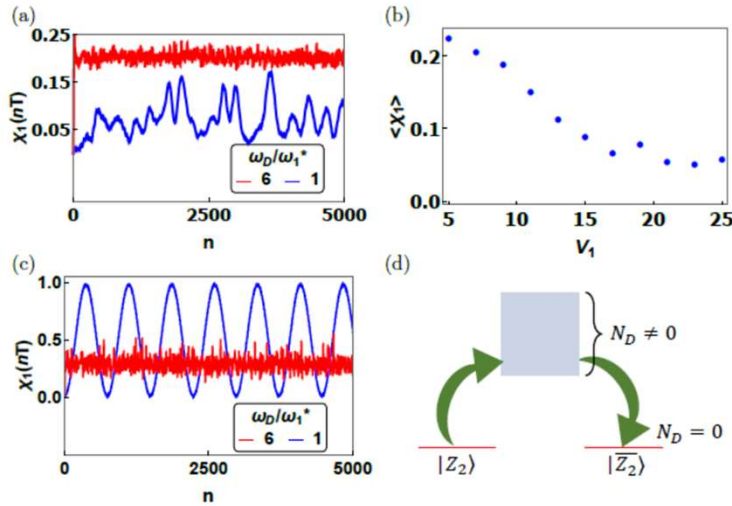


FIG. 3: (a) Plot of $\chi_1(nT)$ as a function of n for $V_1 = 19$ at ω_1^* (blue curve) and $6\omega_1^*$ (red curve) starting from a random frozen state showing lack of ETH predicted thermalization at ω_1^* . (b) Plot of $\langle \chi_1 \rangle$ as a function of V_1 at ω_1^* ; $\langle \chi_1 \rangle$ stays close to its initial value for large V_1 which is consistent with prethermal HSF. (c) Same as in (a) but for initial $|Z_2\rangle$ state showing slow oscillations at ω_1^* . (d) Schematic diagram for the Floquet quasienergies showing doubly degenerate $|Z_2\rangle$ and $|\bar{Z}_2\rangle$ with $N_d = 0$ and other states with $N_d \neq 0$. The arrows indicate transition to $|\bar{Z}_2\rangle$ from $|Z_2\rangle$ using intermediate states with $N_d \neq 0$ leading to slow oscillations. For all plots $V_0 = 10V_2 = 2$, $L = 14$, and all energies are scaled in units of J .

Oscillatory dynamics of frozen states due to residual terms in H_F beyond $H_F^{(1)}$

This requires Z_2 symmetry. Two states with $N_d=0$ which are eigenstates of $H_F^{(1)}$ with same quasienergy.

In addition, it requires fragmentation so that starting from the Z_2 state (which correspond to $N_d=0$), the system does not spread out in Hilbert space; the dynamics receives most significant contribution from states with $N_d = 1$.

Since $\chi_1=0$ (1) for Z_2 and Z'_2 , the oscillations occur between 0 and 1.

The oscillation time scale is determined by higher-order terms in H_F and is the energy split between bonding and antibonding states due to tunneling to $N_d = 1$ sector.

$$|\psi_{B,A}\rangle \equiv |Z_2\rangle \pm |\bar{Z}_2\rangle, \quad H_F |\psi_{B,A}\rangle \approx \hbar(\alpha_s \pm \alpha_d) |\psi_{B,A}\rangle$$

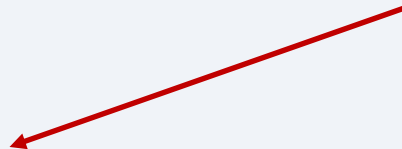
$$\chi_1(nT) \approx \sin^2(\alpha_d nT)$$

This dynamics of frozen states has no analogue in standard HSF in equilibrium

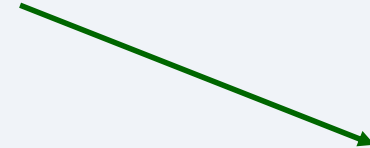
Arresting heating and a two-rate protocol

Arresting heating during a periodic drive

The unbounded growth of entanglement in a driven system



The system reaches and infinite temperature steady state: "heat death"

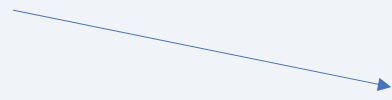


Any information contained in an initial state gets completely scrambled due to rapid spread of the state in the Hilbert in the presence of the drive

Is it possible to arrest this growth?



Counter-diabatic driving



Optimal protocol

Unfortunately both of these are difficult to implement experimentally for a generic ergodic quantum systems

Our suggestion: Use of a two-rate protocol which is experimentally more viable

A class of protocols and exact Floquet flat bands

Consider a generic non-integrable driven Hamiltonian characterized non-commuting operators O_1 and O_2

$$H(t) = \sum_{i=1,2} \lambda_i(t) \hat{O}_i. \quad [\hat{O}_1, \hat{O}_2] \neq 0.$$

We choose a class of two-rate drive protocols with time periods T_1 and T_2

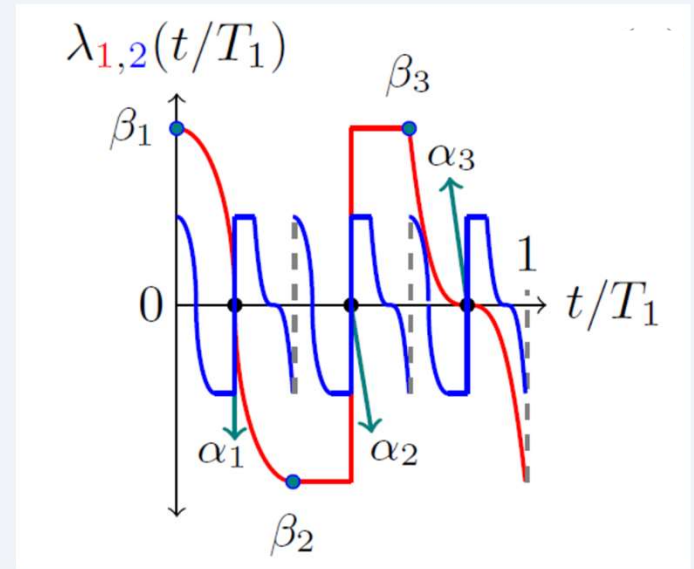
$$T_i = 2\pi/\Omega_i \text{ with } i = 1, 2, \Omega_2 = \nu\Omega_1$$

Familiar examples of such class of protocols with $\nu = 3$

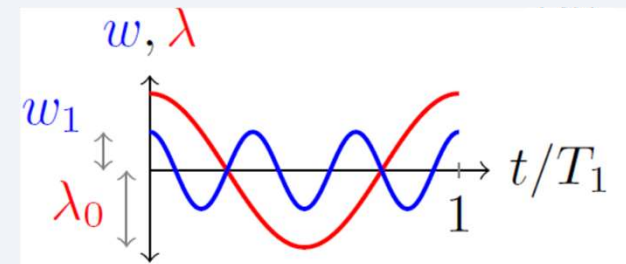
$$\lambda_1(t) = \lambda_0 \cos \Omega_1 t, \quad \lambda_2(t) = w_0 + w_1 \cos \nu \Omega_1 t$$

$$\lambda_1(t) = +(-)\lambda_0 \text{ for } t \leq (>)T_1/2$$

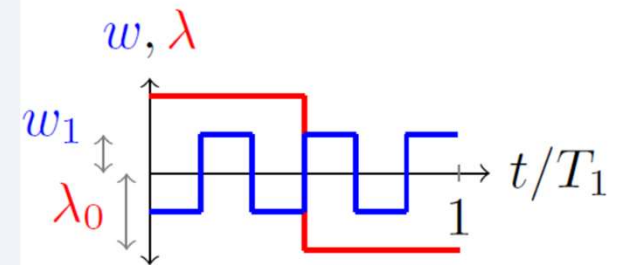
$$\lambda_2(t) = w_0 - [+]w_1 \text{ for } \frac{(m-1)[m]T_1}{2\nu} \leq t < \frac{m[(m+1)]T_1}{2\nu}$$



Cosine



Square Pulse



A simple example: Square pulse protocol with $\nu = 2$

$$H = \lambda_1(t) O_1 + \lambda_2(t) O_2$$

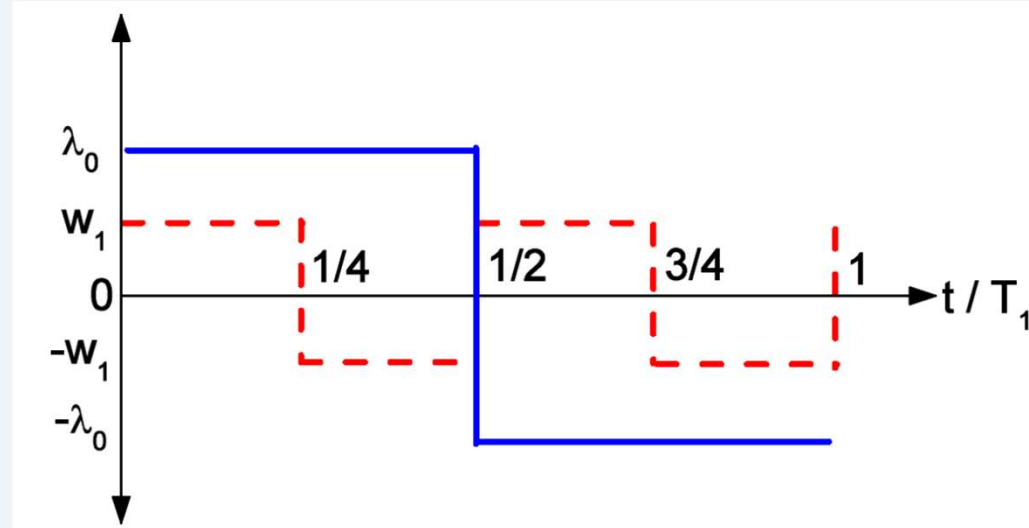
$$\lambda_1(t) = +(-) \lambda_0 \text{ for } t < (>) T_1/2$$

$$\lambda_2(t) = w_1 \text{ for } t < T_1/4 \text{ and } T_1/2 < t < 3 T_1/4 \\ = -w_1 \text{ otherwise}$$

One can write

$$H_0[a,b] = a \lambda_0 O_1 + b w_1 O_2 \quad a, b = 1 \text{ or } -1$$

Note that $H_0[a,b] = -H_0[-a,-b]$



The evolution operator can be written as

$$U(T,0) = e^{-iH_0[-1,-1]T_1/4} e^{-iH_0[-1,1]T_1/4} e^{-iH_0[1,-1]T_1/4} e^{-iH_0[1,1]T_1/4} = I$$

For the square-pulse protocol, this works for any integer ν ; for the cosine protocol, this requires an odd integer $\nu=2p+1$

The method works for any non-commuting operators O_1 and O_2 but requires two rates.

It constitutes exact dynamical localization/freezing in an otherwise ergodic many-body system.

Properties of the chosen protocol for $w_0=0$

They exhibit turning points at $t_j = \beta_j T_1$

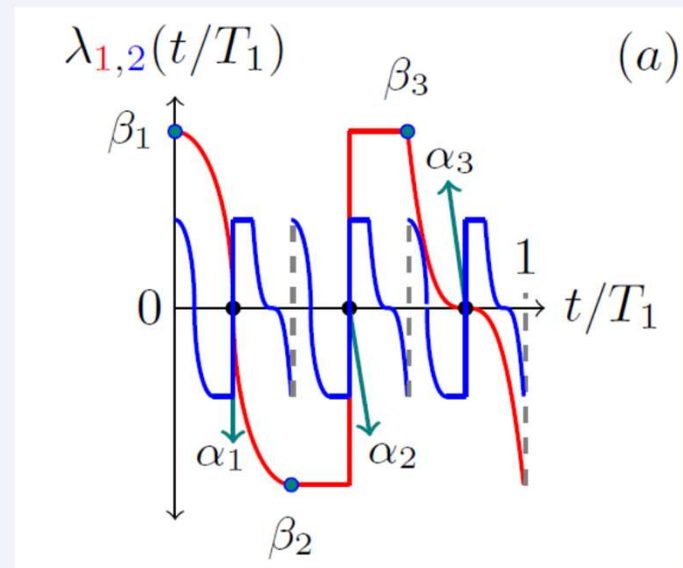
Between any two turning points β_j and β_{j+1} there exist a point $\alpha_j = (\beta_j + \beta_{j+1})/2$ such that $\lambda_i(\alpha_j T_1) = 0$ for $i=1,2$. This ensures

For any $t_0 \leq (\beta_{j+1} - \beta_j) T_1/2$, $H(t)$ satisfies

The evolution operators can therefore be written as, using Suzuki-Trotter decomposition

$$H(\alpha_j T_1) = 0.$$

$$H(\alpha_j T_1 + t_0) = -H(\alpha_j T_1 - t_0)$$



$$U(T_1, 0) = \prod_{k=0 \dots N_0} e^{-iH(t_k)\Delta t/\hbar} = \prod_k U(t_{k+1}, t_k) = \prod_k U_k.$$

$$\Delta t = T_1/(N_0 + 1)$$

This product can be reorganized by grouping U_k s between turning points

$$U(T_1, 0) = \prod_{j=j_{\max}}^1 U(\beta_{j+1}T_1, \beta_{j+1}T_1 - \Delta t)U(\beta_{j+1}T_1 - \Delta t, \beta_{j+1}T_1 - 2\Delta t) \dots U(\alpha_j T_1 + 2\Delta t, \alpha_j T_1 + \Delta t) \\ \times U(\alpha_j T_1, \alpha_j T_1 - \Delta t) \dots U(\beta_j T_1 + 2\Delta t, \beta_j T_1 + \Delta t)U(\beta_j T_1 + \Delta t, \beta_j)$$



The terms in the second line cancel those in the first.

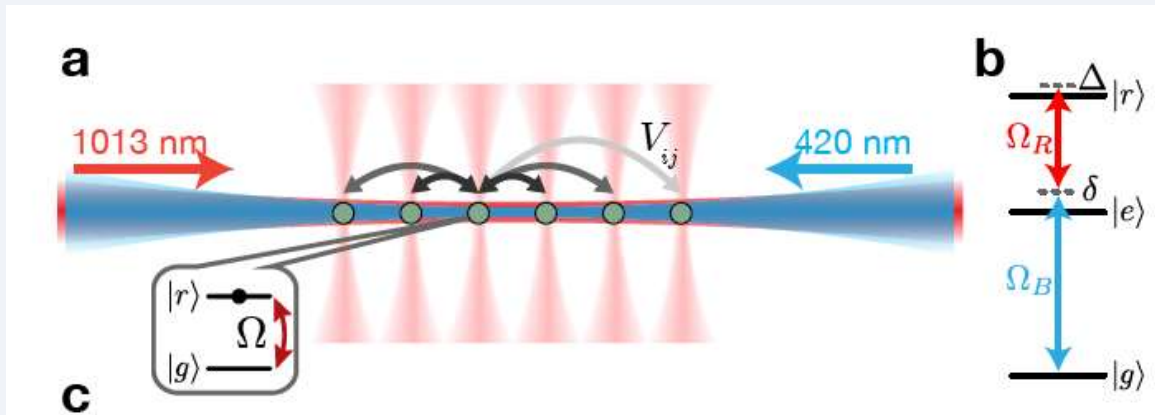
$U(T_1, 0) = I$ for such protocol leading to $E_n^F(T_1) = 0$ for all n



Exact Floquet flat bands for all drive frequencies

Model for studying two-rate dynamics

Rydberg atom arrays



System of ^{87}Rb atoms controllably coupled to their Rydberg excited state.

The van der Waals interaction between two atoms in their excited (Rydberg) states is denoted by V and is a tunable parameter.

One can vary the detuning parameter Δ which allows one to preferentially put the atom in a Rydberg or ground state

H. Bernien et al. Nature 2017

$$\delta \sim 2\pi \times 560 \text{ MHz}$$

$$\Omega_B, \Omega_R \sim 2\pi \times 60, 36 \text{ MHz}$$

$$\Omega = \Omega_B \Omega_R / (2\delta) \sim 2\pi \times 2 \text{ MHz.}$$

$$|g\rangle = |5S_{1/2}, F = 2, m_F = -2\rangle$$

$$|r\rangle = |71S_{1/2}, J = 1/2, m_J = -1/2\rangle$$

Effective low-energy description

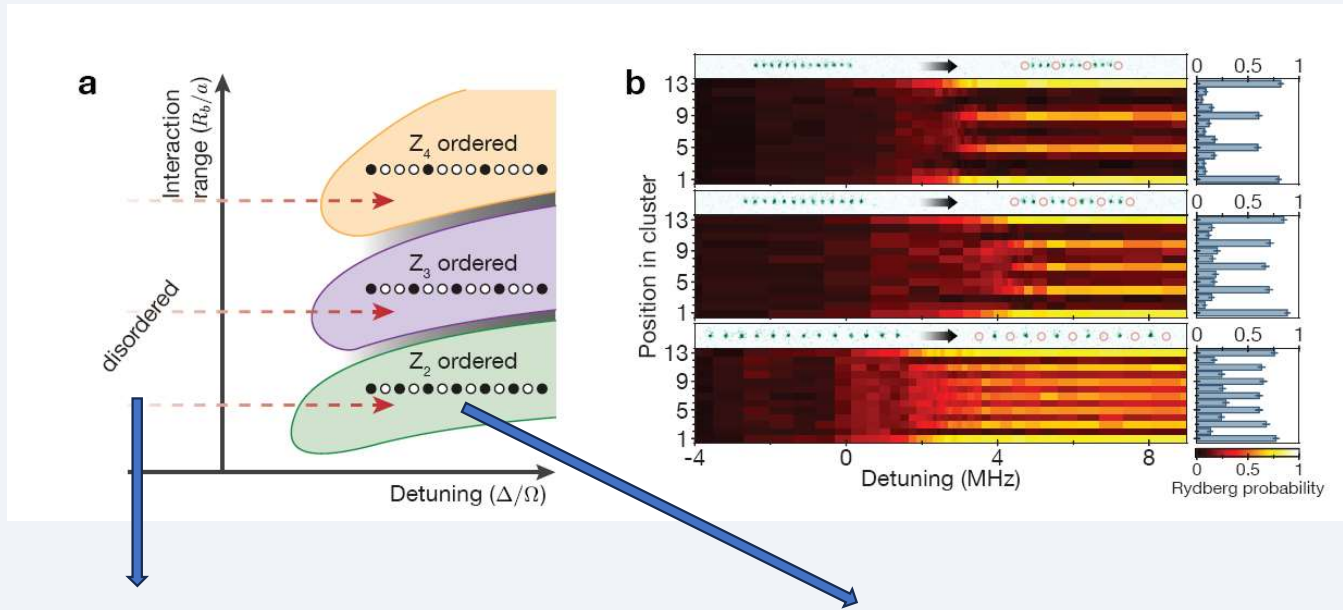
$$\frac{\mathcal{H}}{\hbar} = \sum_i \frac{\Omega_i}{2} \sigma_x^i - \sum_i \Delta_i n_i + \sum_{i < j} V_{ij} n_i n_j,$$

$$n = (1 + \sigma^z) / 2$$

$$V_{ij} = V_0 / |r_{ij}|^6$$

V_0 can be tuned so that Rydberg excitations in neighbouring sites are forbidden.

H. Bernien et al. Nature 2017



Rydberg vacuum ($|0\rangle$) for $\Delta \gg \Omega$ and $\Delta < 0$

Z_2 ($|Z_2\rangle$) state for $\Delta \gg \Omega$ and $\Delta > 0$.



These states are separated by an Ising transition

Similar to the transition found in tilted optical lattice

S. Sachdev et al, PRB 66, 075128 (2002), P Fendley et al PRB 69, 075106 (2004)

Mapping to a constrained model

$$\frac{\mathcal{H}}{\hbar} = \sum_i \frac{\Omega_i}{2} \sigma_x^i - \sum_i \Delta_i n_i + \sum_{i < j} V_{ij} n_i n_j,$$

Two states per site: Natural spin $\frac{1}{2}$ representation

$$\sigma_\ell^z = 2n_\ell - 1, \quad \sigma_\ell^{x(y)} = (i)(d_\ell + (-)d_\ell^\dagger).$$

Rydberg blockade on neighboring sites: $V_{i,i+1} \gg \Delta, \Omega \gg V_{i,i+2}$

$$P_\ell = (1 - \sigma_\ell^z)/2$$

A up-spin (Rydberg excitation) can be created on a site if and only if there are no up-spins (excitations) on the neighboring sites

$$\frac{\mathcal{H}}{\hbar} = \sum_i \frac{\Omega_i}{2} \sigma_x^i - \sum_i \Delta_i n_i + \sum_{i < j} V_{ij} n_i n_j,$$



$$\begin{aligned} H_{\text{spin}} &= -w \sum_\ell P_{\ell-1} \sigma_\ell^x P_{\ell+1} + \lambda/2 \sum_\ell \sigma_\ell^z \\ &= \sum_\ell (-w \tilde{\sigma}_\ell^x + \lambda/2 \sigma_\ell^z) \end{aligned}$$

Drive the system by making λ and w periodic function of time with frequencies Ω_1 and Ω_2 : $\Omega_2 = 3 \Omega_1$

Dynamics around exact flat bands

Floquet bands and the spectral form factor

We study the PXP Hamiltonian describing Rydberg atom array

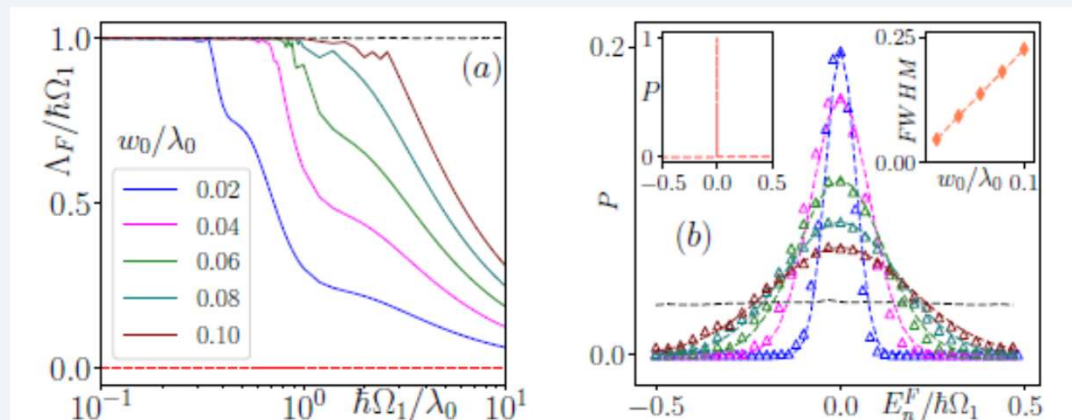
$$H_R = \lambda_1(t) \sum_j \sigma_j^z + \lambda_2(t) \sum_j \tilde{\sigma}_j^x$$

Use exact diagonalization (ED) to find the eigenspectrum of U and hence H_F

Non-perturbative regime: $w_1 = \lambda_1 = \Omega_1$ and $w_0 < w_1$

Floquet bandwidth Λ_F as a function of Ω_1 and for $\nu=3$.

For single rate drive Floquet ETH predicts $\Lambda_F = h\Omega_1$



Plot of distribution, P , of the Floquet eigenenergies within the first Floquet Brillouin zone for $\Omega_1 = w_1 = \lambda_1$.

For $w_0=0$, P is a delta function peaked at zero while Floquet ETH predicts a flat distribution

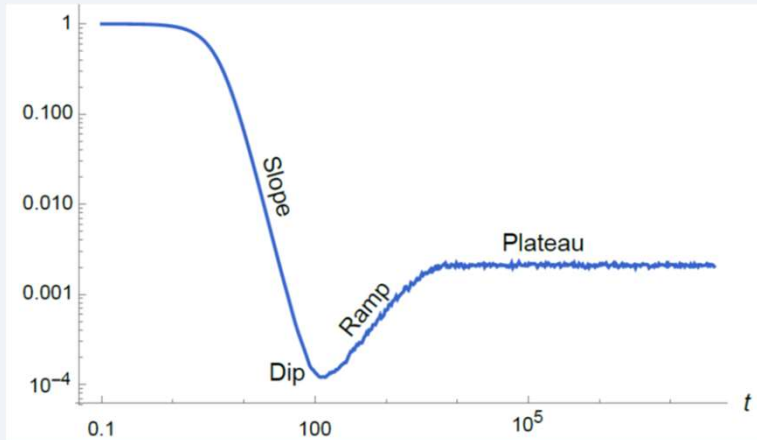
Red dashed line $\rightarrow w_0=0$ where one has exact Floquet flat band

Black dashed line \rightarrow single rate drive protocol with $w_1=0$ and $w_0=1$

The nature of the Floquet band is qualitatively different for a wide range of w_0 around the exact flat band limit.

Strong deviation from prediction of Floquet ETH (realized for single rate drive protocol).

Spectral form factor



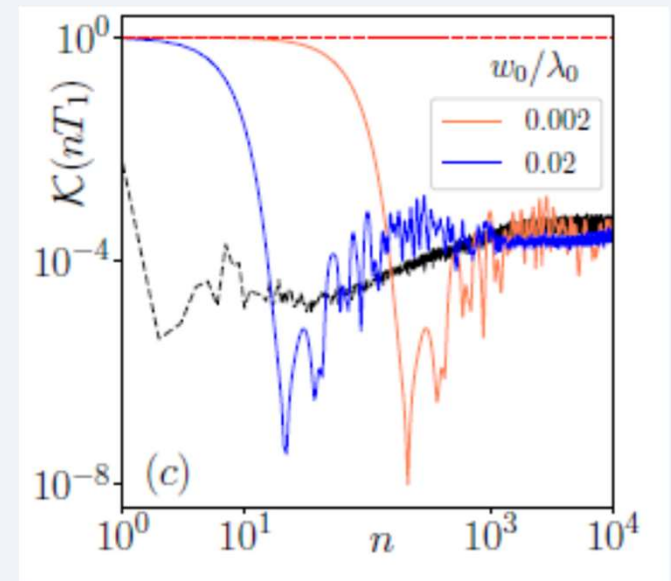
*SYK model for
N=26 fermions*



$$\mathcal{K}(nT_1) = \frac{1}{\mathcal{D}^2} \sum_{p,q=1}^{\mathcal{D}} e^{i(E_p^F - E_q^F)nT_1/\hbar}$$



L=16, two rate protocol



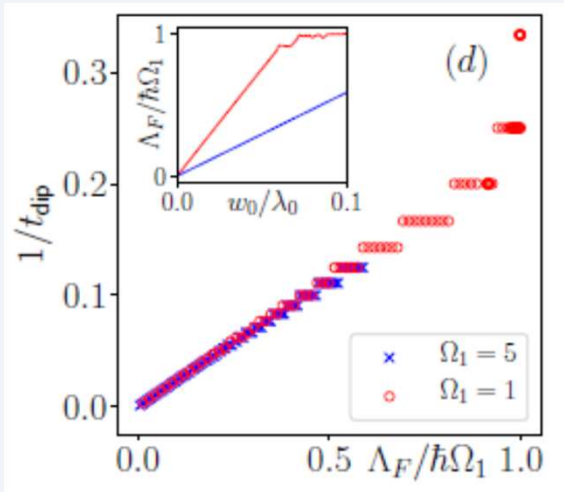
For the two-rate protocol, the dip time can be extended for small w_0

The ramp region signifying thermalization always occur after the dip

This indicates a large prethermal timescale and slow thermalization at small w_0

Numerically, we find $1/t_{dip} \sim \Lambda_F$ and hence w_0 : w_0 provides a knob for slowing down thermalization

Dependence of dip time on Floquet bandwidth



Exact numerics confirms the linear dependence

The steps occur due to integer nature of n_d

To obtain an estimate of the dip time we note the following:

1) At short times, the spectral form factor can be written as

$$\mathcal{K}(nT_1) \simeq 1 - (nT_1)^2 \sum_{p,q} (E_p^F - E_q^F)^2 / (2\hbar^2 \mathcal{D}^2).$$

2) The sum over eigenstates can be converted to an integral over energy gaps using a density of states ρ

$$\int_{-\Lambda_F/2}^{\Lambda_F/2} \rho d\epsilon = \mathcal{D} = \sum_{m \in \Lambda}$$

3) We choose $\rho = \rho_0 \Lambda_F^{-1} f(\epsilon/\Lambda_F)$ $\rho_0 \sim \mathcal{D}$

4) Using this DOS, one finds

$$\begin{aligned} \mathcal{K}(nT_1) &\simeq 1 - \frac{(nT_1 \Lambda_F)^2 \rho_0}{2\mathcal{D}\hbar^2} \int_{-1/2}^{1/2} dx f(x) x^2 \\ &= 1 - c_0 (nT_1 \Lambda_F / \hbar)^2 \end{aligned}$$

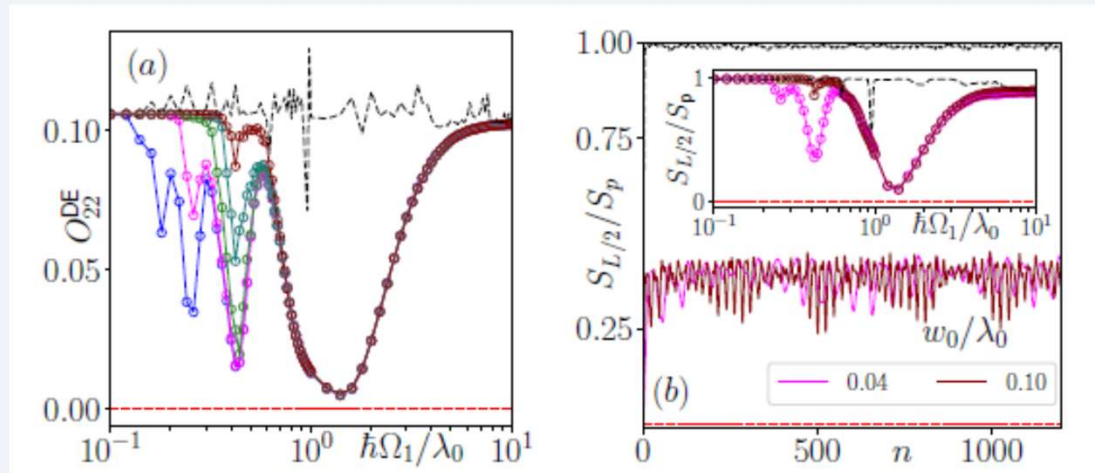
5) This allows one to estimate the dip time

$$t_{\text{dip}} = n_d T_1, \text{ where } n_d \sim \text{Int}[\hbar / (T_1 \Lambda_F)]$$

Correlation and entanglement

Correlation function

$$O_{j2}^{\text{DE}} = \text{Tr}[\rho_D \hat{n}_j \hat{n}_{j+2}]$$



*Half chain entanglement
Starting from the Rydberg
vacuum (all spin-down
state)*

The entanglement and the correlation function stays at their initial value in the flat band limit: perfect freezing.

Both the entanglement and correlation shows a broad dip over a wide range of frequency for finite w_0

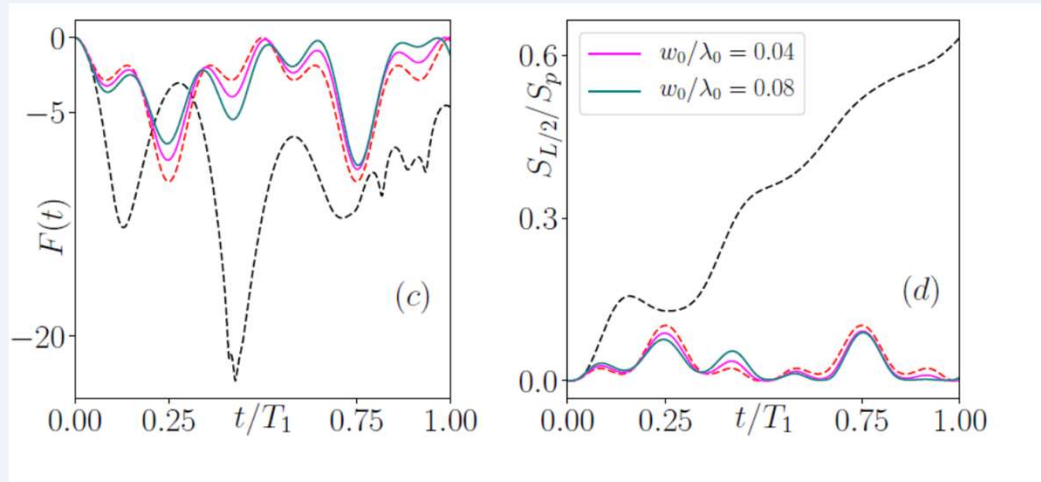
For the single rate drive (black curve), both of these quantities obey the Floquet ETH predicted result. The correlation stays nears its diagonal ensemble predicted value while the entanglement saturates to its Page value

The half-chain entanglement, for two rate-protocol at finite w_0 , saturates to a much lower value signifying a lower spread of the initial state in the Hilbert space.

Micromotion

Fidelity $F(t)$

$$\ln |\langle \psi(0) | \psi(t) \rangle|^2$$



**Half-chain Entanglement
 $S_{L/2}(t)$**

Rapid decay of fidelity and growth of entanglement for single rate drive protocol (black-dashed line)

In contrast, $F(t)$ remains close to zero for two-rate drive protocols both zero and finite w_0

The growth of entanglement is also much smaller for the two-rate protocol

The spread of the driven state in the Hilbert space and hence heating is drastically reduced.

For $w_0=0$, one has an exact symmetry in micromotion $O(t) = O(T_1-t)$ for all t .

The dynamics involves coherent reversal of excitations and is reminiscent of spin echoes.

Analytical result at high drive amplitude

Floquet Perturbation theory (single rate protocol for Rydberg model)

Uses w/λ as the small parameter: accurate for large drive amplitude and intermediate drive frequencies.

At the zeroth order, the evolution operator receives contribution from the σ^z term.

$$U_0(t,0) = e^{i\lambda t \sum_j \sigma_j^z/2} \quad \text{for } t \leq T/2,$$

$$= e^{i\lambda(T-t) \sum_j \sigma_j^z/2} \quad \text{for } T/2 \leq t \leq T.$$

$$\langle m|U_0(t,0)|n\rangle = \delta_{mn} e^{im\lambda t/2} \quad \text{for } t \leq T/2,$$

$$= \delta_{mn} e^{i\lambda(T-t)m/2} \quad \text{for } T/2 \leq t \leq T,$$

Using standard perturbation theory, one obtains the first order contribution to H_F as follows

$$U_1(T,0) = -i \int_0^T dt H_I(t)$$



$$\langle m|U_1(T,0)|n\rangle = \delta_{m,n+s} \frac{2w}{\lambda s} \left(e^{i\lambda s T/2} - 1 \right)$$

$s = \pm 1.$

Thus one can write

$$U_1(T,0) = \sum_m \sum_j \sum_{s_j=\pm 1} c_{s_j}^{(1)} |m\rangle \langle m + s_j|,$$

$$c_s^{(1)} = \frac{4iw}{\lambda} \sin(\lambda T/4) e^{i\lambda T s/4},$$

This yields the first order Floquet Hamiltonian

$$H_F^{(1)} = -w \frac{\sin(\gamma)}{\gamma} \sum_j [\cos(\gamma) \tilde{\sigma}_j^x + \sin(\gamma) \tilde{\sigma}_j^y],$$

Magnus in rotated frame

Resummation of the standard Magnus expansion

Application to two-rate protocol

$$H_F^{(1)} = \frac{w_0 \sin(\lambda_0 T_1/2)}{\lambda_0 T_1/2} \sum_{j,s=\pm} \tilde{\sigma}_j^s e^{-i\lambda_0 T_1 s/2}$$

The drive amplitude $2\lambda_0 \gg w_0 w_1$ for validity of the perturbation theory.

Floquet Hamiltonian vanishes at $w_0=0$; consistent with exact flat band.

The presence of second order term is different from analogous expansion in single-rate protocol where only odd order terms are present.

This is due presence of chirality operator C_0 for single rate protocol satisfying

$$C_0 = \prod_j \sigma_j^z$$

$$\{H_F, C_0\} = 0.$$

This property is absent for the two-rate protocol for finite w_1 and w_0

$$H_F^{(2)} = \frac{2w_0 w_1 \mathcal{C}}{\lambda_0} \sum_j (\sigma_j^z + (\tilde{\sigma}_j^+ \tilde{\sigma}_{j+1}^- + \text{h.c.}))$$

$$\mathcal{C} = 6[2 \sin(x/6) - 2 \sin(x/3) + \sin(x/2)]/x - 1,$$

$$x = 2\lambda_0 T_1/\hbar.$$

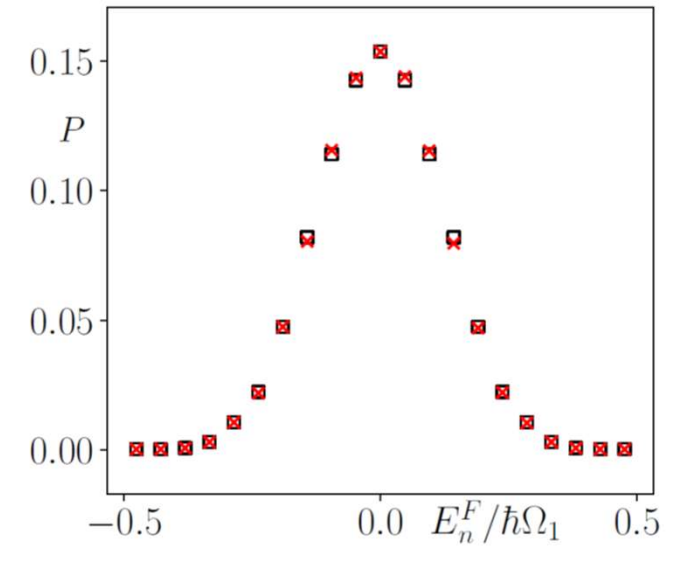


FIG. 6. Plot of the eigenvalue distribution P within the first FBZ for $\hbar\Omega_1/w_0 = 15$, $w_1/w_0 = 0.1$, and $\lambda_0/w_0 = 20$. The red crosses show results from second order FPT while the black open squares indicate those from exact numerics obtained using ED. For both plots $L = 24$, $K_0 = 0$ and we have used square-pulse protocol with $\nu = 3$.

Out-of-time correlators

$$C(mT) = \langle [n_j(mT), n_i(0)]^2 \rangle = 2(1 - F(mT))$$

$$F(mT) = \langle n_j(mT) n_i(0) n_j(mT) n_i(0) \rangle$$



Provides information about spread of correlation between sites of the driven chain

Generic properties

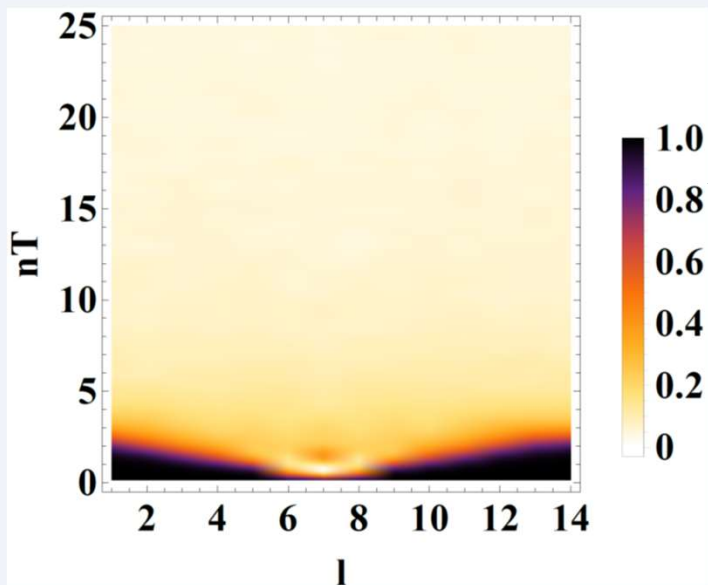
At the initial time, $C=0$ and $F=1$.

As the operator spreads, $F \rightarrow 1$ and $C \rightarrow 0$

This spread of this correlation at initial times is linear and is bounded by the Lieb-Robinson velocity.

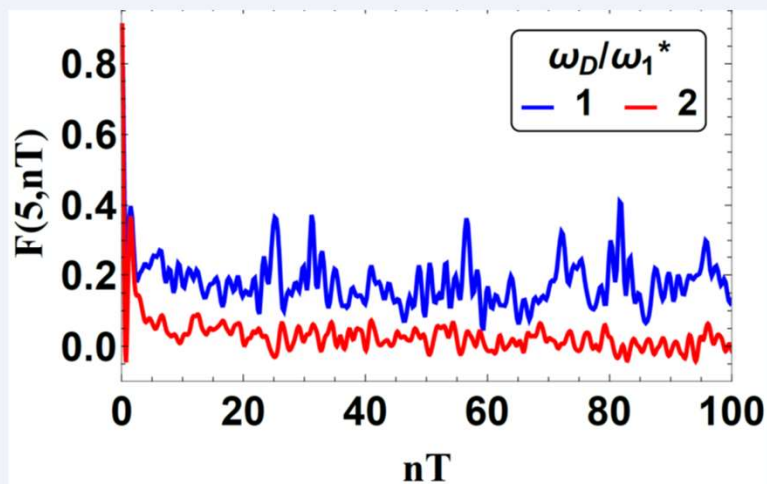
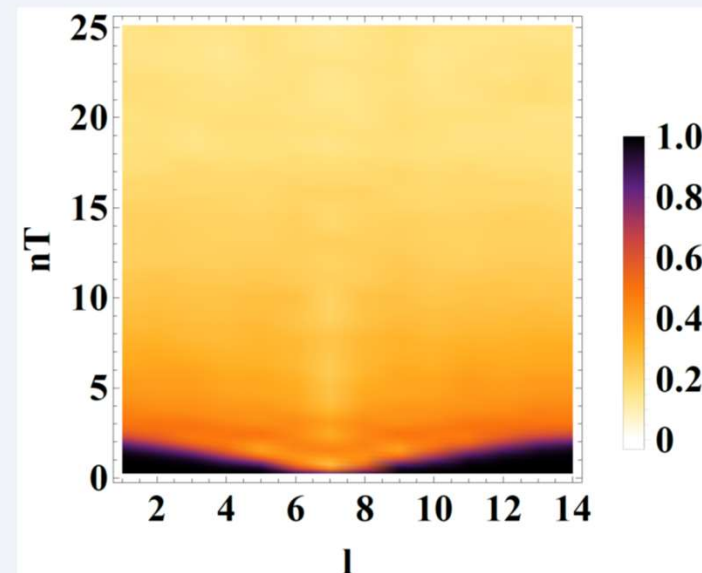
For ergodic systems, F shows a rapid convergence to its steady state value ($F \sim 1$).

For fragmented systems, the late time values of F depends on the initial condition.



Away from special frequency

At a special frequency



Dynamics of F

No. of drive cycles after which F reaches near-zero (0.01) value on the farthest site.

